Università degli Studi di Padova
Dipartimento di Fisica e Astronomia "Galileo Galilei"
Corso di Laurea Triennale in Fisica

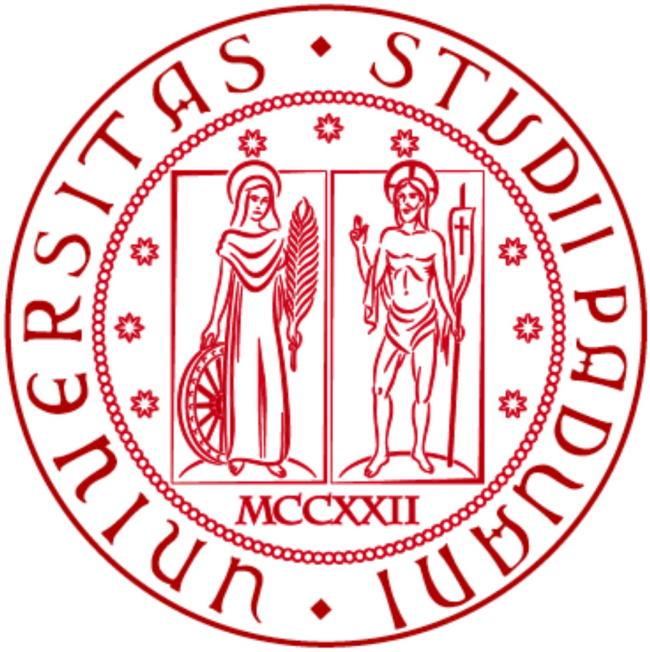

Sensitivity to the neutrino oscillation parameters with the JUNO experiment

Studente: Nicola Garlet
Matricola: 1051549

Relatore: Alberto Garfagnini
Co-relatore: Marco Grassi

Anno accademico: 2014/'15

Contents

List of Figures

1 Introduction

The neutrino oscillation is a phenomenon where a neutrino created with a particular leptonic flavour - electronic, muonic or tauonic - can later be measured with a different flavour. The probability of measuring a particular flavour varies periodically as the neutrino propagates through space. This phenomenon implies that the neutrino has a non-zero mass, which was not included in the original Standard Model. Neutrino oscillation derives from a mixture of the neutrino flavour eigenstates and mass eigenstates: each leptonic state is a different superposition of the three mass states.
The thesis takes inspiration from the Jiangmeng Underground Neutrino Observatory (JUNO) experiment, which will take place in China starting from 2020: JUNO is a 20 kton multi-purpose 700m underground liquid scintillator detector with excellent energy resolution and large fiducial volume and whose main purpose is to verify which is the true neutrino mass hierarchy. The JUNO detector offers also opportunities for many important topics in neutrino physics and astro-particle physics.
This bachelor thesis aims to analyze how the sensitivity for some of the neutrino oscillation parameters varies with the energy resolution of an experiment.

2 Neutrino oscillation parameters

2.1 The neutrino oscillation

The Standard Model of Particle Physics is a successful theory which not only unifies the electromagnetic and weak interactions but also explains almost all the phenomena of this nature observed at or below the electroweak scale. When this theory was first formulated by Weinberg in 1967 [1], the neutrinos were assumed to be massless and hence there would be no lepton flavour mixing. But just one year later the solar neutrinos were observed by Davis and others [2], and a deficit of their flux as compared with the prediction from the standard solar model was also established by Bahcall and others [3, 4]. Such an anomaly turned out to be solid evidence for new physics beyond the standard model, because it was found to be attributed to the neutrino oscillation - a spontaneous and periodic change from one neutrino flavour to another, which does not take place unless neutrinos have finite masses and lepton flavours are mixed.
Flavour oscillations can therefore serve as a powerful tool to study the intrinsic properties of massive neutrinos [5].

2.2 The $\bar{\nu}_e$ survival probability

In a nuclear reactor, anti-neutrinos are mainly produced via beta decay of the fission products of four radioactive isotopes, ^{235}U, ^{238}U, ^{239}Pu and ^{241}Pu, in the fuel. The number of anti-neutrinos produced per fission depends on their energy $E_{\bar{\nu}_e}$ [6]

$$\begin{aligned}\phi_{\bar{\nu}_e} =& f_{^{235}U} \exp(0.870 - 0.160E_{\bar{\nu}_e} - 0.091E_{\bar{\nu}_e}^2) \\ &+ f_{^{239}Pu} \exp(0.896 - 0.239E_{\bar{\nu}_e} - 0.0981E_{\bar{\nu}_e}^2) \\ &+ f_{^{238}U} \exp(0.976 - 0.162E_{\bar{\nu}_e} - 0.0790E_{\bar{\nu}_e}^2) \\ &+ f_{^{241}Pu} \exp(0.793 - 0.080E_{\bar{\nu}_e} - 0.1085E_{\bar{\nu}_e}^2) \end{aligned} \quad (1)$$

where f_k denotes the relative fission contribution of the isotope k in a reactor fuel. Although f_k varies overtime as the fuel is burned, it can be approximated for this type of experiments with the average value of the relative fission contributions: $f_{^{235}U} = 0.58$, $f_{^{239}Pu} = 0.30$, $f_{^{238}U} = 0.07$ and $f_{^{241}Pu} = 0.05$ [7].
The event rate of anti-neutrinos with energy $E_{\bar{\nu}_e}$ (MeV) at a reactor of P (GW) thermal power is then expressed as $\frac{dN}{dE_{\bar{\nu}_e}} = \frac{P}{\sum_k f_k \epsilon_k} \phi(E_{\bar{\nu}_e}) \cdot 6.24 \times 10^{21}$, where ϵ_k is the released energy per fission of the isotope k: $\epsilon_{^{235}U} = 201.7MeV$,$\epsilon_{^{239}Pu} = 210.0MeV$, $\epsilon_{^{238}U} = 205.0MeV$ and $\epsilon_{^{241}Pu} = 212.4MeV$ [8]. The numerical factor comes from unit conversion, $1GW/MeV = 6.24 \times 10^{21}$.

This rate is then modulated by oscillation. The $\bar{\nu}_e$ survival probability is expressed as

$$\begin{aligned} P_{ee} =& |\sum_{i=1}^{3} U_{ei} \exp(-i\frac{m_i^2 L}{2E_i}) U_{ei}^*|^2 \\ =& 1 - \cos^4(\theta_{13}) \sin^2(2\theta_{12}) \sin^2(\Delta_{21}) \\ & - \sin^2(2\theta_{13}) \sin^2(|\Delta_{31}|) \\ & - \sin^2(\theta_{12}) \sin^2(2\theta_{13}) \sin^2(\Delta_{21}) \cos(2|\Delta_{31}|) \\ & + \alpha \sin^2(\theta_{12}) \sin^2(2\theta_{13}) \sin(2\Delta_{21}) \sin(2|\Delta_{31}|) \end{aligned} \quad (2)$$

where U_{ei} is the neutrino mixing matrix element relating the electron neutrino to the mass eigenstate ν_i. The variables m_i and E_i are the mass and energy of the corresponding mass eigenstate, while θ_{ij} represents a neutrino mixing angle. α represents the mass hierarchy: it is $\alpha = +1$ for the normal hierarchy (NH), while $\alpha = -1$ for the inverted hierarchy (IH). The oscillation phases Δ_{ij} are defined as $\Delta_{ij} \equiv \frac{\Delta m_{ij}^2 L}{4E_\nu}$, with $\Delta m_{ij}^2 = m_i^2 - m_j^2$ and it has been assumed $E_{\bar{\nu}_e} \sim E_1 \sim E_2 \sim E_3$ [9].
JUNO will use free protons as targets to detect electronic anti-neutrinos via the inverse neutron beta decay (IBD) process $\bar{\nu}_e + p \rightarrow e^{-}_{+} + n$, where p and n are the proton and the neutron, respectively. The threshold neutrino energy of this process is $E_{thr} = m_n - m_p + m_e = 1.81$MeV, and the cross section is [10]

$$\begin{aligned} \sigma_{IBD} &= 0.0952 \cdot (\frac{E_e p_e}{1\text{MeV}}) \times 10^{-42} cm^2 \\ &= 0.0952 \cdot (\frac{(E_{\bar{\nu}} - (m_n - m_p)) \cdot \sqrt{(E_{\bar{\nu}} - (m_n - m_p))^2 - m_e^2}}{1\text{MeV}}) \times 10^{-42} cm^2 \end{aligned} \quad (3)$$

where E_e and p_e are the energy and momentum of the positron, neglecting the kinetic energy of the proton and the neutron for a MeV scale anti-neutrino. The positron's energy is roughly $E_e \sim E_{\bar{\nu}} - (m_n - m_p) \sim E_{\bar{\nu}} - 1.30$MeV [9].

3 The JUNO experiment

JUNO [5] is a multi-purpose neutrino experiment. It has been proposed in 2008 to determine the neutrino mass hierarchy by detecting reactor antineutrinos from the Daya Bay nuclear power plant (NPP) [7, 11, 12, 13], thus formerly known as "Daya Bay II experiment". The mass hierarchy determination requires equal baselines from the detector to all reactor cores to avoid cancellation of the oscillation dephasing effect. Due to the complex and unclear layout of the future nuclear power plants in the neighborhood, the location of the experiment was moved to Jiangmen in the Guangdong province in August 2012, and named JUNO in 2013. The site location is optimized to have the best sensitivity for the mass hierarchy determination, which is at 53 km from both the Yangjiang and Taishan NPPs [14]. Data taking is expected in 2020.
The JUNO detector consists of a central detector, a water Cherenkov detector and a muon tracker. A schematic view of the JUNO detector is shown in Figure 1 [5]. The central detector is a liquid scintillator based detector of 20 kton fiducial mass with an designed energy resolution of $3\%/\sqrt{E(\text{MeV})}$. The central detector is submerged in a water pool to be shielded from natural radioactivity from the surrounding rock and air. The water pool is equipped with Photomultiplier Tubes (PMTs) to detect the Cherenkov light from cosmic muons, acting as a veto detector. On top of the water pool, there is another muon detector to accurately measure part of the muon tracks crossing the detector from the top.

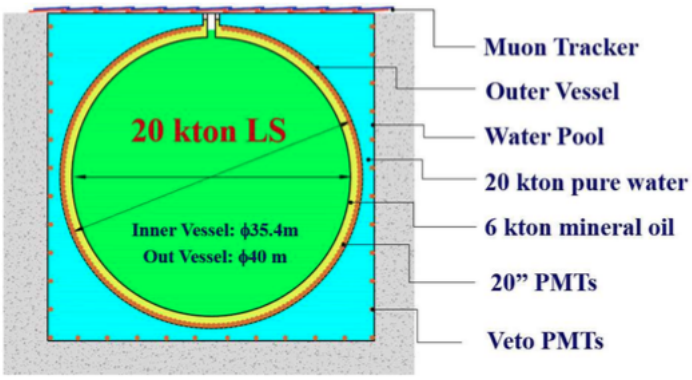

Figure 1: A schematic view of the JUNO detector.

After the discovery of non-zero θ_{13} mixing angle in recent reactor [15, 16, 17, 18] and accelerator [19, 20] neutrino experiments, the present status of the standard three-flavor neutrino oscillation [21, 22, 23, 24, 25, 26] can be summarized as follows:

- three non-zero mixing angles [27] θ_{12}, θ_{23}, and θ_{13} in the MNSP [28, 29] lepton mixing matrix have been measured with the precision from 4% to 10%,
- two independent mass-squared differences $|\Delta m^2_{31}| = |m^2_3 - m^2_1|$ (or $|\Delta m^2_{32}| = |m^2_3 - m^2_2|$) and $\Delta m^2_{21} = m^2_2 - m^2_1$ have been measured with the precision better than 4% [27],
- the neutrino mass hierarchy (i.e., sign of the mass-squared difference Δm^2_{31}) is unknown,
- the octant of the mixing angle θ_{23} (i.e., $\theta_{23} < \pi/4$ or $\theta_{23} > \pi/4$) is unknown,
- the leptonic CP-violating phase δ in the MNSP matrix is unknown.

Therefore, the determination of the neutrino mass hierarchy and octant of the mixing angle θ_{23}, as well as the measurement of the leptonic CP-violating phase constitutes the main focus of future neutrino oscillation experiments. The neutrino mass hierarchy (MH) answers the question whether the third generation (ν_3 mass eigenstate) is heavier or lighter than the first two generations (ν_1 and ν_2). As shown in Figure 2, the normal mass hierarchy (NH) refers to $m_3 > m_1$ and the inverted mass hierarchy (IH) refers to $m_3 < m_1$.
The determination of the MH has profound impacts on our understanding of the neutrino physics, neutrino astronomy and neutrino cosmology [5].

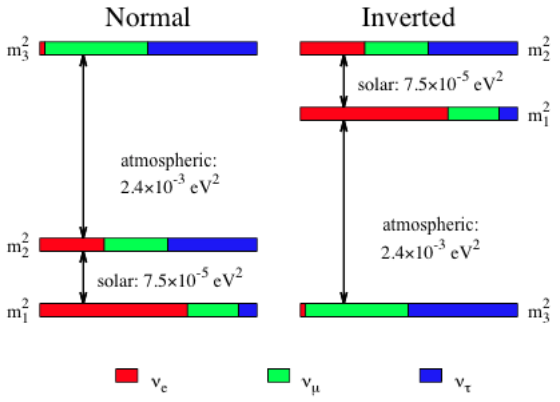

Figure 2: Illustration for the patterns of normal and inverted neutrino mass hierarchies.

4 Sensitivity to neutrino oscillation parameters

The aim for this thesis is to study the neutrino oscillation and in particular to understand how the sensitivity for the neutrino oscillation parameters $\sin^2(2\theta_{12})$, Δm^2_{12} and $\sin^2(2\theta_{13})$ varies with the energy resolution of the experiment. The sensitivity for a measured quantity is defined as $sensitivity = \frac{1\sigma}{measured\ quantity}$.
In Table 1 the PDG values for the three parameters amove mentioned are displayed.

Parameter	PDG value	PDG error
$sin^2(2\theta_{12})$	0.846	2.5%
Δm^2_{12}	7.53	2.4%
$sin^2(2\theta_{13})$	0.093	8.6%

Table 1: The PDG values for the parameters with the corresponding uncertainty.

First of all, three functions have been implemented: the neutrinos flux from the NPPs $\phi_{\bar{\nu}_e}(E_{\bar{\nu}_e})$ (eq(1) - plot in Figure 3), the $\bar{\nu}_e$ cross section for the inverse beta decay $\sigma_{IBD}(E_{\bar{\nu}_e})$ (eq(3) - plot in Figure 4) and the $\bar{\nu}_e$ survival probability $P_{ee}(E_{\bar{\nu}_e})$ for the NH case (eq(2) - plot in Figure 5).
It is worth noticing that while $\phi_{\bar{\nu}_e}$ decreases exponentially with the anti-neutrinos energy, σ_{IBD} increases more than linearly: therefore, its product is bell-shaped. This is then convoluted with P_{ee}, which is featured by two types of oscillations: a larger one, due to θ_{12}, and a smaller one, due to θ_{13}.

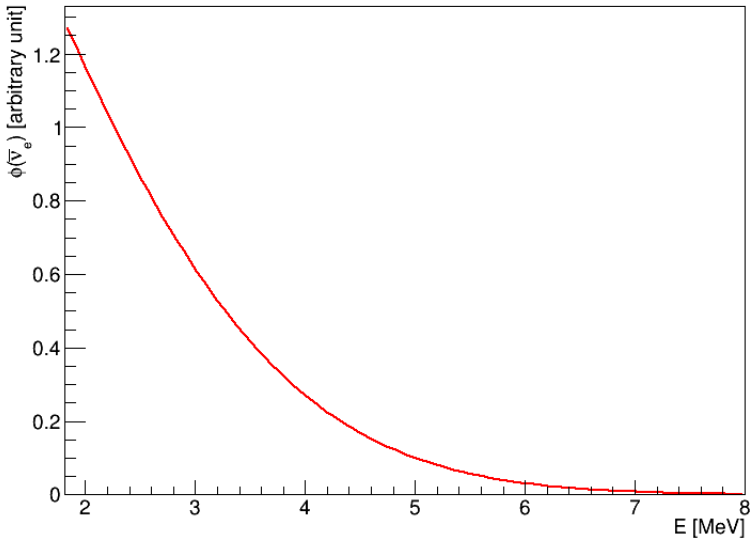

Figure 3: The $\bar{\nu}_e$ flux from the NPPs reactors.

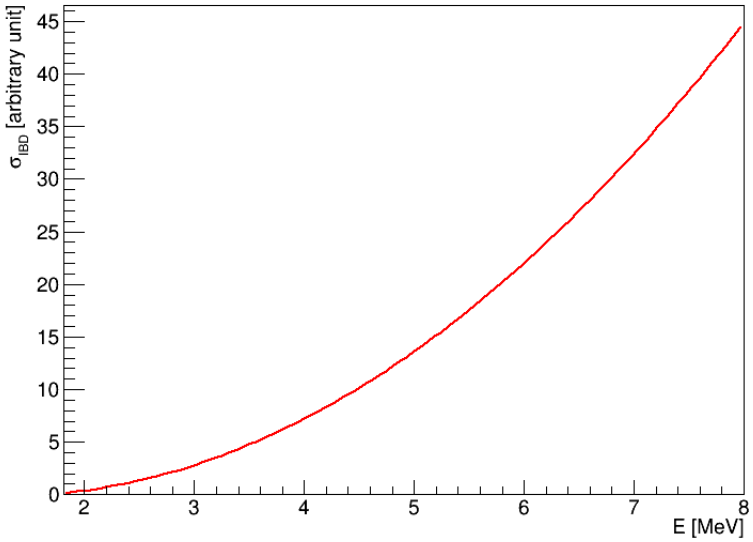

Figure 4: $\bar{\nu}_e$ cross section for the inverse beta decay as a function of the anti-neutrino energy.

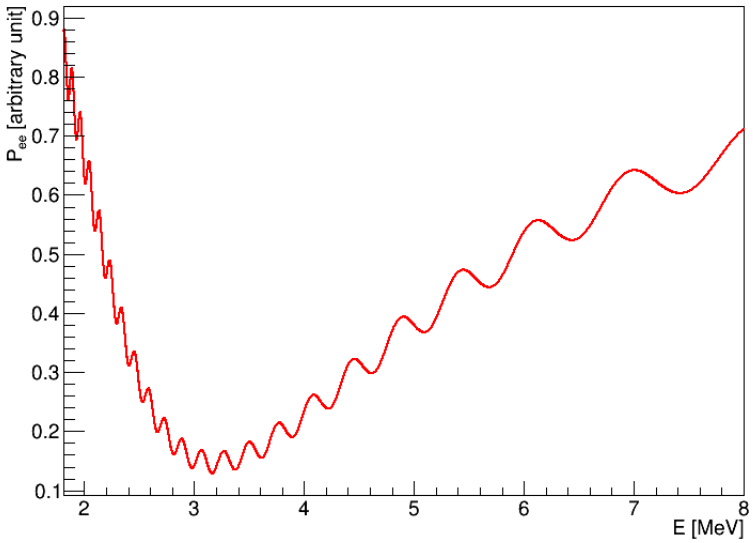

Figure 5: The $\bar{\nu}_e$ survival probability for the JUNO experiment baseline, assuming NH.

Given these three functions, the formula for the $\bar{\nu}_e$ spectrum $\frac{dN}{dE_{\bar{\nu}_e}}(E_{\bar{\nu}_e})$ at the JUNO location, modulated by the oscillation probability $P_{ee}(E_{\bar{\nu}_e})$, can be implemented as the product of them. $\frac{dN}{dE_{\bar{\nu}_e}} \times P_{ee}$ is plotted in Figure 6.

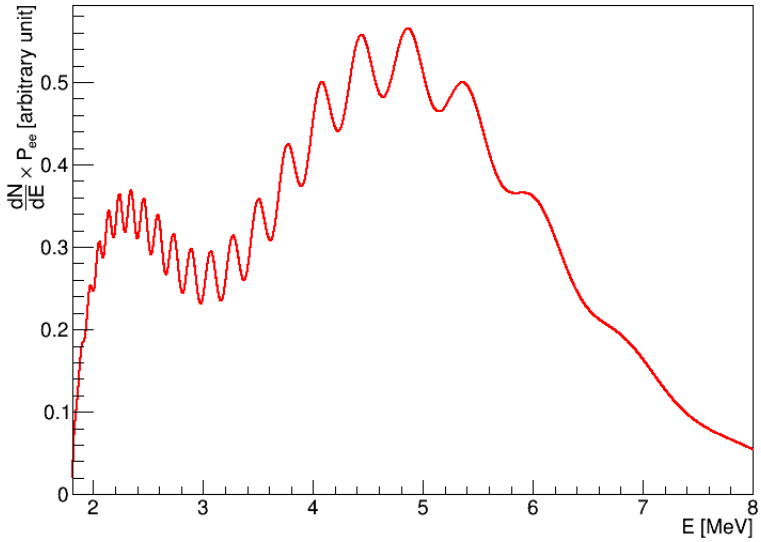

Figure 6: The $\bar{\nu}_e$ spectrum $\frac{dN}{dE_{\bar{\nu}_e}} \times P_{ee}$ for the JUNO experiment baseline (NH).

The resulting function has then been used as a probability density function, therefore normalizing it (Figure 7), and its cumulative function has been constructed (Figure 8) in order to generate data following the given spectrum via a Monte Carlo method. Precisely, what was generated is a set of numbers with a uniform distribution between 0 and 1, then converted into energy values thanks to the inverse function of the cumulative function. This way a set of likely data for an experiment with infinite resolution has been produced (Figure 9). The number of generated data is 100000 and the number of used bins is 256.

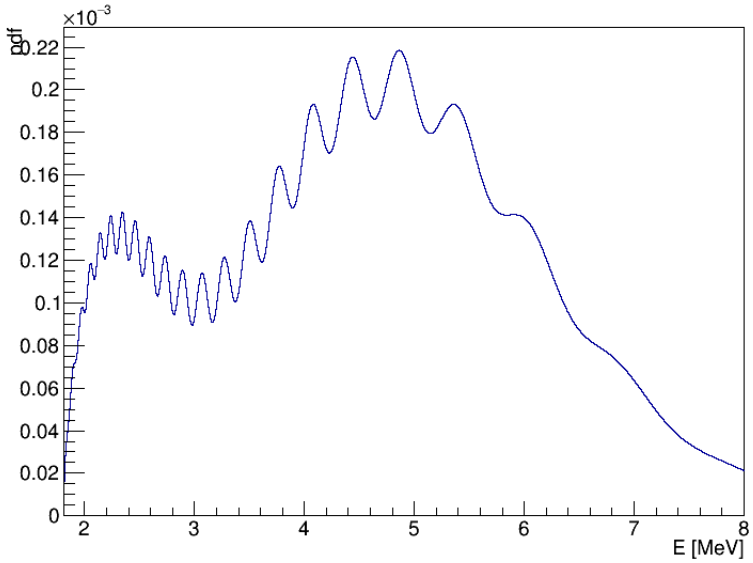

Figure 7: The pdf for the data to be generated.

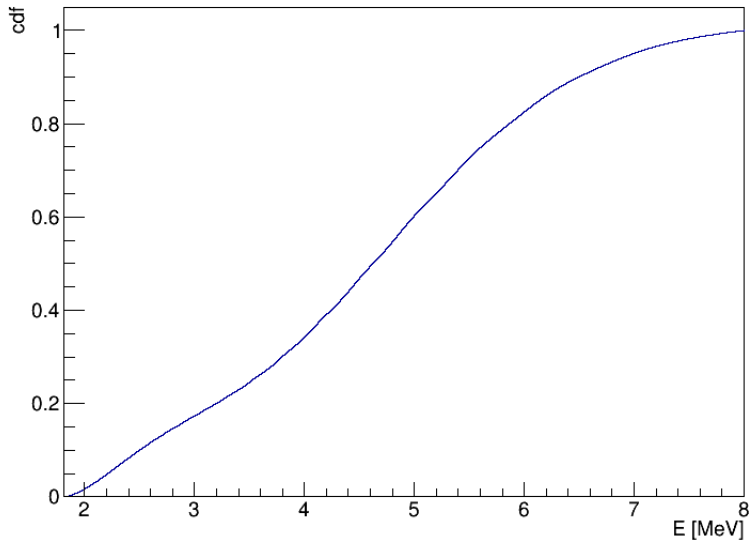

Figure 8: The cdf used by the Monte Carlo method to generate the data.

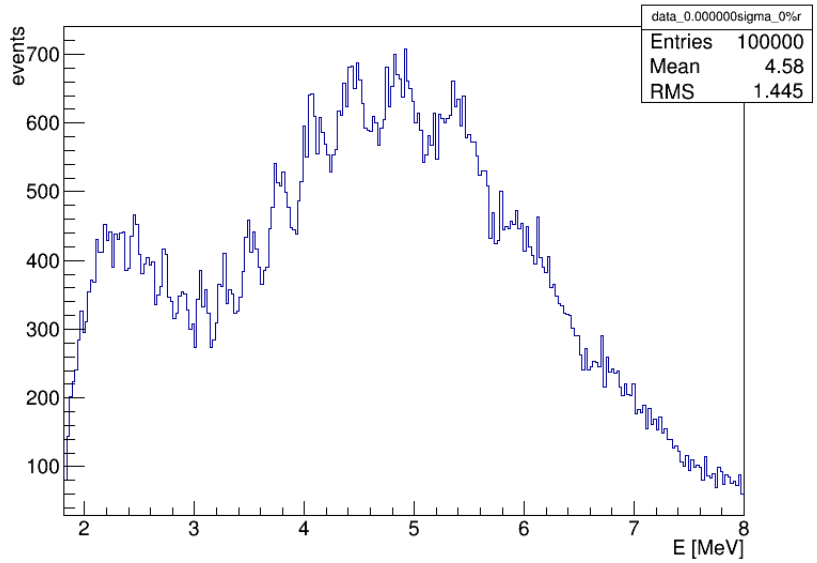

Figure 9: Data generated with the PDG values for $\sin^2(2\theta_{12})$, Δm^2_{12} and $\sin^2(2\theta_{13})$ for an ideal infinite resolution experiment.

After this, in order to plot likely data, that is with the resolution effect, other data have been generated in the same way but with the introduction, as a last step, of a gaussian smearing with another Monte Carlo method. Precisely speaking, once generated each energy value with infinite resolution, a gaussian distribution has been implemented with the value created E as its mean and $resolution \cdot \sqrt{E}$ as its standard deviation to generate a new value following this gaussian distribution and this is the kept value. The used resolution ratios are 2%, 4%, 6%, 8% and 10%. An example of smeared data set, that is with a 6% resolution, is plotted in Figure 10.

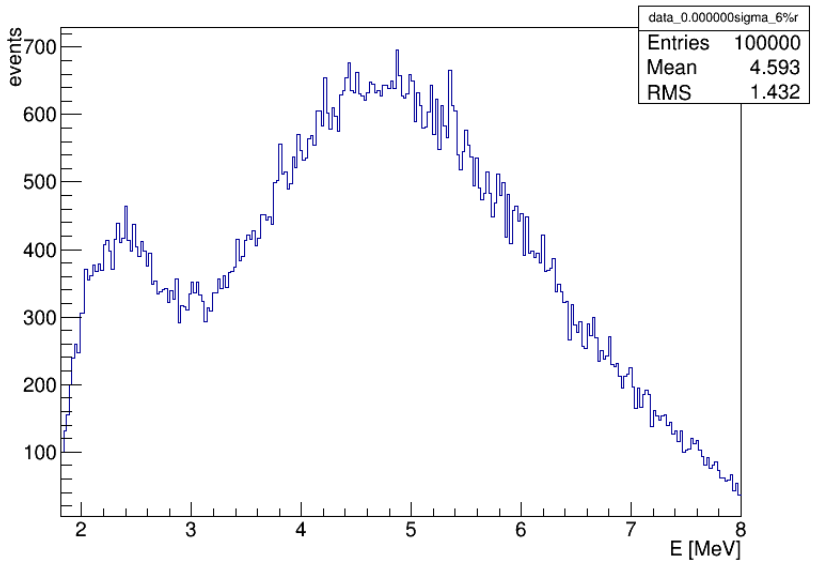

Figure 10: Data generated with the PDG values for $\sin^2(2\theta_{12})$, Δm^2_{12} and $\sin^2(2\theta_{13})$ for a 6% resolution experiment.

What has just been described was done with the values for $\sin^2(2\theta_{12})$, Δm^2_{12} and $\sin^2(2\theta_{13})$ given by the Particle Data Group (PDG).

After this, the same thing has been done, varying one parameter between -3σ and $+3\sigma$ with an 0.33σ interval, while keeping the other two fixed with the PBD value. This way data sets were obtained for each of the three parameters and for each resolution level. The number of generated data is no longer 100000 in these cases, since the variation of a parameter implies a change in the anti-neutrino spectrum. Instead, the number of data for each case is

$$N_{events} = 100000 \times \frac{integral(current\ \bar{\nu}_e\ spectrum)}{integral(PDG\ values\ \bar{\nu}_e\ spectrum)}$$

In Figure 11, Figure 12 and Figure 13 some superimposed plots, with infinite resolution and 6% resolution, are displayed for this procedure on $\sin^2(2\theta_{12})$, Δm^2_{12} and $\sin^2(2\theta_{13})$ respectively.

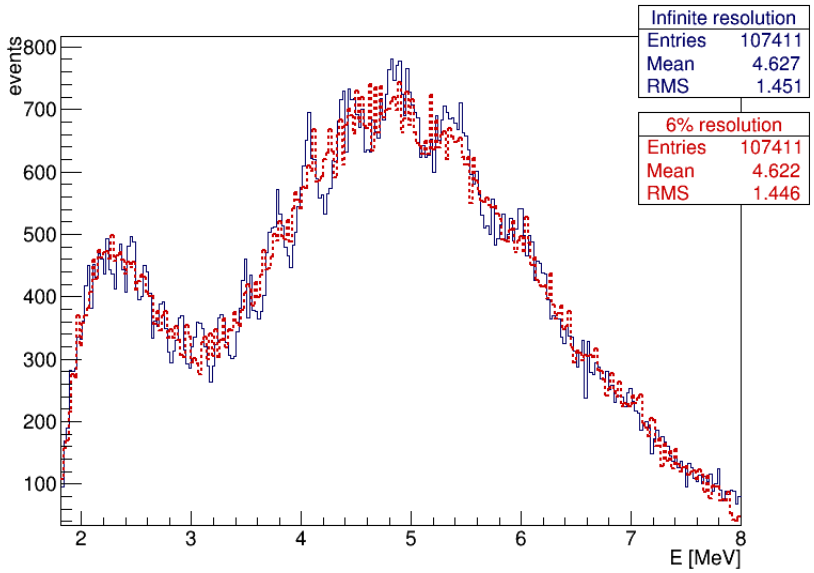

Figure 11: Data with $\sin^2(2\theta_{12}) + 1.33\sigma_{PDG}$ with an infinite resolution (continuous line) and a 6% resolution (dotted line).

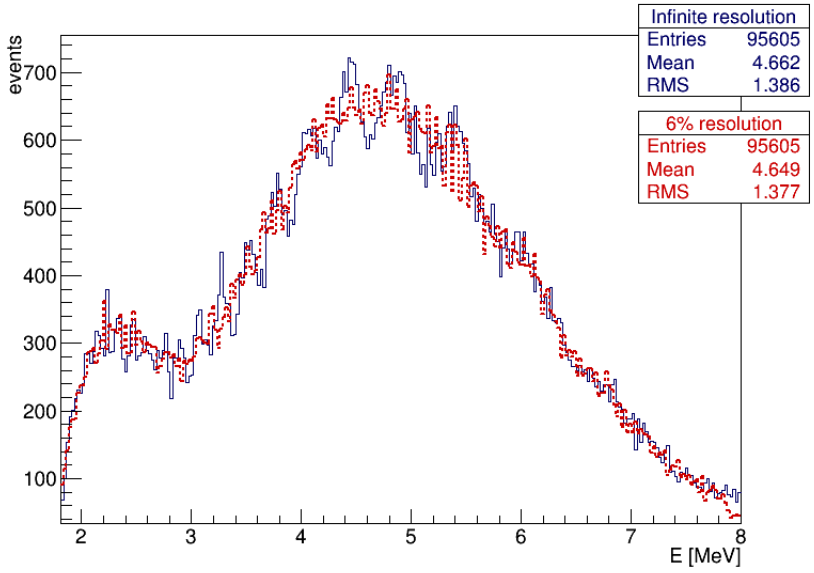

Figure 12: Data with $\Delta m^2_{12} - 2\sigma_{PDG}$ with an infinite resolution (continuous line) and a 6% resolution (dotted line).

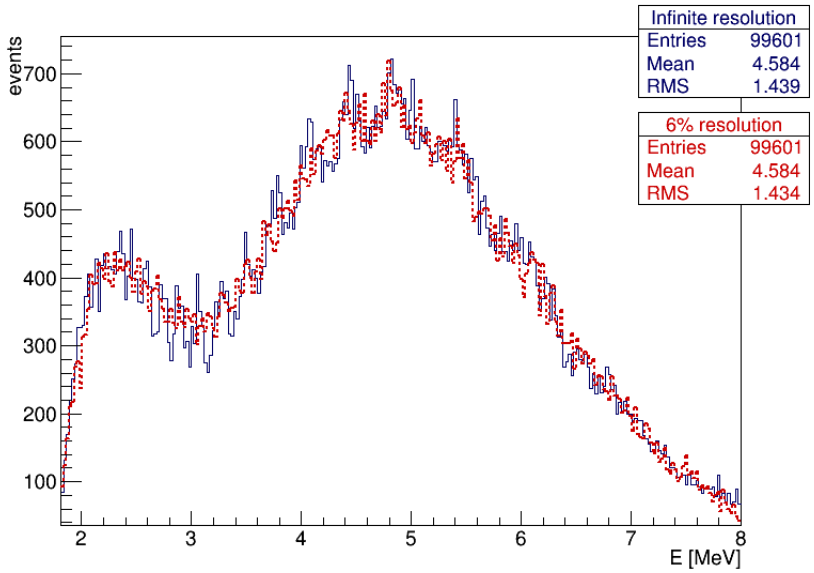

Figure 13: Data with $\sin^2(2\theta_{13}) - 1\sigma_{PDG}$ with an infinite resolution (continuous line) and a 6% resolution (dotted line).

At this point a normalized χ^2 was constructed for each parameter for each of the 6 resolution levels, thus obtaining for each of the three parameters 6 sets of points with an almost parabolic trend if plotted as functions of the parameter value, given one resolution level. The purpose is to find the minimum of χ^2/N varying one parameter. In Figure 14 and Figure 15 examples of $\frac{\chi^2}{N}$ are plotted for $\sin^2(2\theta_{12})$ and Δm^2_{12} respectively.

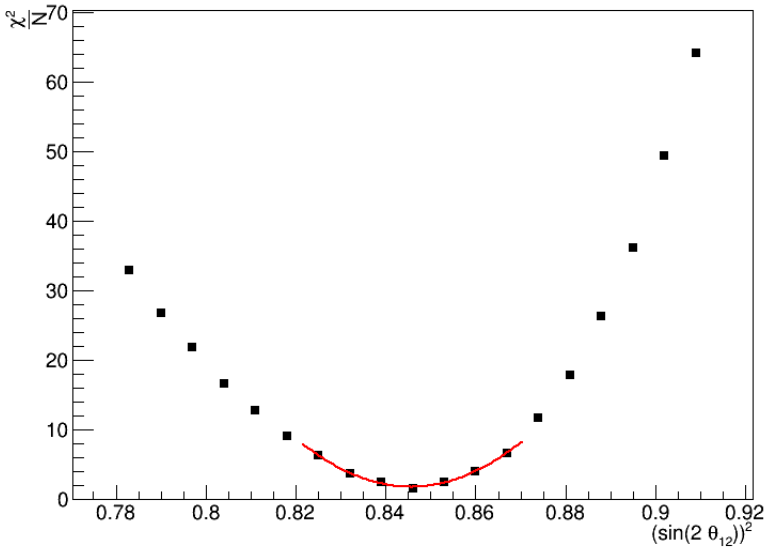

Figure 14: Normalized χ^2 for different values of $\sin^2(2\theta_{12})$ with a 4% resolution.

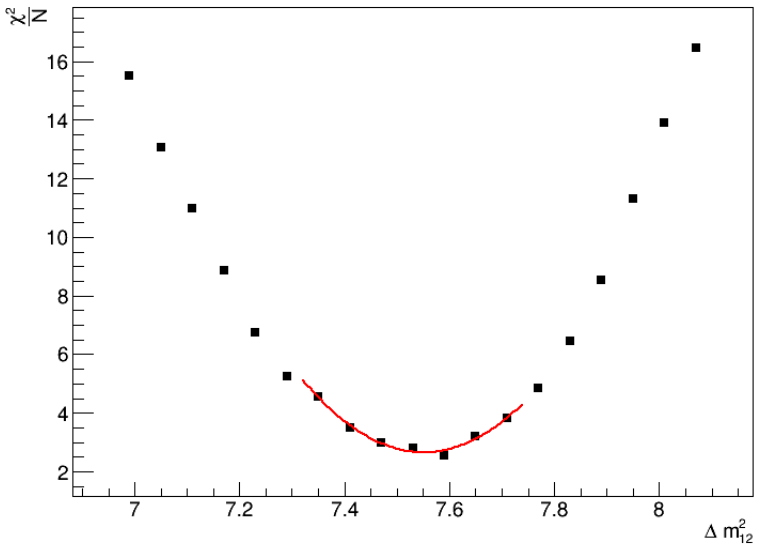

Figure 15: Normalized χ^2 for different values of Δm^2_{12} with a 8% resolution.

While the χ^2 points for $\sin^2(2\theta_{12})$ and Δm^2_{12} are well aligned, the alignment for $\sin^2(2\theta_{13})$ is poorer. This is due to the fact that the first two parameters are related to the larger oscillation in $\frac{dN}{dE_{\bar{\nu}_e}} \times P_{ee}$ (Figure 6 at page 8) while the latter parameter is related to the smaller oscillation. Thus, the statistics is more important for the quality of the χ^2 for $\sin^2(2\theta_{13})$.
At this point the sets could be fitted with a parabola for values of the specific parameter not farther than 1 σ from the PDG value for $\sin^2(2\theta_{12})$ and Δm^2_{12} and for each value for $\sin^2(2\theta_{13})$. This way the minimum value of the fitting function could be found. Dividing the width corresponding to an unitary increment of $\frac{\chi^2}{N}$ from its minimum value by the minimum value itself, the sensitivity for each resolution level for each parameter could be obtained. The sensitivities for $\sin^2(2\theta_{12})$ and Δm^2_{12} are displayed in Figure 16, while the one for $\sin^2(2\theta_{13})$ is displayed in Figure 17.

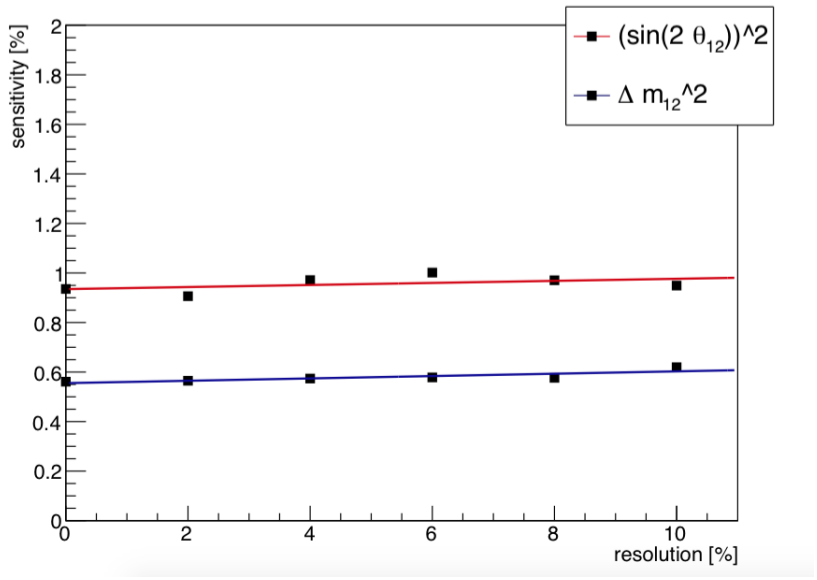

Figure 16: The sensitivity for the parameters $\sin^2(2\theta_{12})$ and Δm^2_{12}.

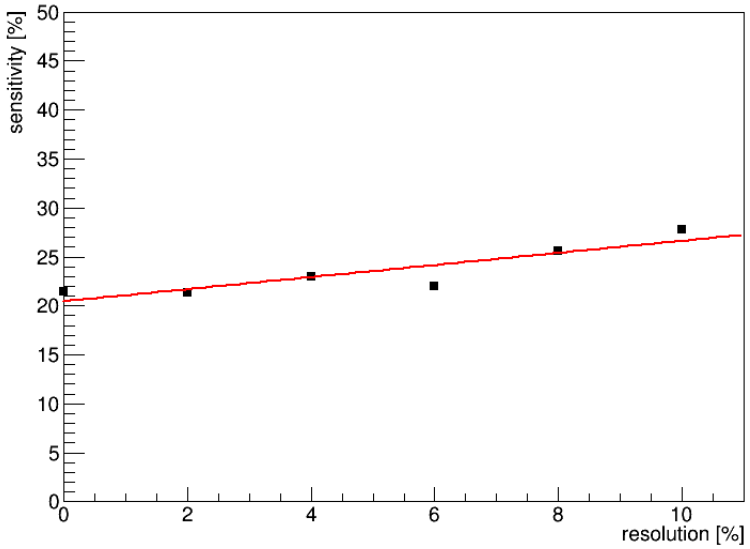

Figure 17: The sensitivity for the parameter $\sin^2(2\theta_{13})$.

Parameter	$\frac{d(sensitivity)}{d(resolution)}$
$\sin^2(2\theta_{12})$	0.0048 ± 0.0015
Δm^2_{12}	0.0042 ± 0.0039
$\sin^2(2\theta_{13})$	0.62 ± 0.16

Table 2: The sensitivity vs. resolution increment for each parameter.

In Table 2 the evaluated $\frac{d(sensitivity)}{d(resolution)}$ for each parameter is displayed. It can be seen that the sensitivity does not vary remarkably with the resolution, while it is mainly driven by the statistics. Even the parameter $\sin^2(2\theta_{13})$, which has the worst sensitivity among the three parameters since it is related to the smaller oscillation and is even more sensitive to the statistics, keeps its sensitivity in a small range between 20% and 25% for reasonable resolution ratios.

5 Conclusions

In this thesis the neutrino oscillation has been studied considering JUNO, a next generation experiment. JUNO has been planned and optimized to measure the mass hierarchy and therefore it is situated at the minimum of the oscillation curve. Even so, thanks to the great mass of the detector, in the first 5 years of data taking a high statistics of neutrinos interactions are expected, in the order of 10^5. The sensibility for the parameters $\sin^2(2\theta_{12})$ and Δm^2_{12} has thus been studied: the result is that, for the JUNO experiment, it is almost constant versus the energy resolution, while it is almost completely driven by the number of events. This analysis also aimed to verify how JUNO could measure the parameter $\sin^2(2\theta_{13})$, another typical parameter studied at reactors experiments. The results are that, even though JUNO has not been designed to measure this parameter, this measure does not vary significantly with the energy resolution of the experiment. JUNO is capable of measuring $\sin^2(2\theta_{13})$, but the expected precision for this parameter will not be competitive with the Data Bay estimee [5, 15]. Part of the 8 Daya Bay detectors are indeed located 1.6km away from the reactors, where the probability of disappearence of the electronic anti-neutrinos due to θ_{13} is maximum. Instead, the distance between JUNO and its sources has been chosen to be 53km in order to maximise the sensitivity to the mass hierarchy. At this distance, the electronic anti-neutrinos probability of disappearence is dominated by θ_{12}, while the contribute due to θ_{13} is less relevant.
The JUNO experiment has an expected energy resolution level of 3%. Given this value, the used numbers

of events and the results of this analysis, the expected sensitivity for each of these three parameters is given in Table 3.

Parameter	**Expected sensitivity**
$\sin^2(2\theta_{12})$	$(0.579 \pm 0.005)\%$
Δm^2_{12}	$(0.95 \pm 0.01)\%$
$\sin^2(2\theta_{13})$	$(22.3 \pm 0.5)\%$

Table 3: The expected sensitivity for each parameter.

This analysis has been made with the NH assumption, but the results do not depend on the neutrino mass hierarchy.

References

[1] S.Weinberg. Phys. Rev. Lett. 19, 1264 (1967).

[2] R. Jr. *et al.* Phys. Rev. Lett. 20, 1205 (1968).

[3] J.N.Bahcall *et al.* Phys. Rev. Lett. 20, 1209 (1968).

[4] J.N.Bahcall *et al.* Rev. Mod. Phys. 54, 767 (1982).

[5] F.An *et al.*, "Neutrino physics with JUNO." [arXiv:1507.05613v1], 2015.

[6] P.Vogel and J.Engel, "Neutrino electromagnetic form-factors." Phys. Rev. D 39 (1989) 3378 [INSPIRE].

[7] L.Zhan *et al.*, "Determination of the neutrino mass hierarchy at an intermediate baseline." Phys. Rev. D 78, 111103 (2008) [arXiv:0807.3203 [hep-ex]].

[8] P. Huber and T. Schwetz, "Precision spectroscopy with reactor anti-neutrinos." Phys. Rev. D 70 (2004) 053011 [hep-ph/0407026] [INSPIRE].

[9] S.Ge *et al.*, "Determination of mass hierarchy with medium baseline reactor neutrino experiments." JHEP05(2013)131 [arXiv:1210.8141], 2013.

[10] P.Vogel and J.F.Beacom, "Angular distribution of neutron inverse beta decay, $\bar{\nu} + p \to e^+ + \nu$." Phys. Rev. D 60 (1999) 053003 [hep-ph/9903554] [INSPIRE].

[11] L.Zhan *et al.* Phys. Rev. D 79, 073007 (2009) [arXiv:0901.2976 [hep-ex]].

[12] Y.Wang, "Talk at ICFA seminar." http://www.conf.slac.stanford.edu/icfa2008/Yifang_Wang_102808.pdf, 2008.

[13] J.Cao, "Talk at Neutrino Telescope." http://neutrino.pd.infn.it/NEUTEL09/Talks/Cao.pdf, 2009.

[14] Y.F.Li *et al.* Phys. Rev. D 88, 013008 (2013) [arXiv:1303.6733 [hep-ex]].

[15] F.P.An *et al.* Phys. Rev. Lett. 108, 171803 (2012) [arXiv:1203.1669 [hep-ex]]. [Daya Bay Collaboration].

[16] F.P.An *et al.* Chin. Phys. C 37, 011001 (2013) [arXiv:1210.6327 [hep-ex]]. [Daya Bay Collaboration].

[17] Y.Abe *et al.* Phys. Rev. Lett. 108, 131801 (2012) [arXiv:1112.6353 [hep-ex]]. [Double Chooz Collaboration].

[18] J.K.Ahn *et al.* Phys. Rev. Lett. 108, 191802 (2012) [arXiv:1204.0626 [hep-ex]]. [RENO Collaboration].

[19] K.Abe *et al.* Phys. Rev. Lett. 107, 041801 (2011) [arXiv:1106.2822 [hep-ex]]. [T2K Collaboration].

[20] P.Adamson *et al.* Phys. Rev. Lett. 107, 181802 (2011) [arXiv:1108.0015 [hep-ex]]. [MINOS Collaboration].

[21] F.Capozzi *et al.* Phys. Rev. D 89, 093018 (2014) [arXiv:1312.2878 [hep-ph]].

[22] D.V.Forero *et al.* Phys. Rev. D 90, no. 9, 093006 (2014) [arXiv:1405.7540 [hep-ph]].

[23] M.C.Gonzalez-Garcia *et al.* JHEP 1411, 052 (2014) [arXiv:1409.5439 [hep-ph]].

[24] G.L.Fogli *et al.* Phys. Rev. D 86, 013012 (2012) [arXiv:1205.5254 [hep-ph]].

[25] D.V.Forero *et al.* Phys. Rev. D 86, 073012 (2012) [arXiv:1205.4018 [hep-ph]].

[26] M.C.Gonzalez-Garcia *et al.* JHEP 1212, 123 (2012) [arXiv:1209.3023 [hep-ph]].

[27] K.A.Olive *et al.*, "Neutrino mass, mixing and oscillations." Chin. Phys. **C38**, 090001, 2014. [Particle Data Group Collaboration].

[28] Z.Maki *et al.* Prog. Theor. Phys. 28, 870 (1962).

[29] B.Pontecorvo. Sov. Phys. JETP 26, 984 (1968) [Zh. Eksp. Teor. Fiz. 53, 1717 (1967)].